Volume 6 | Number 12 | 21 June 2016 | Pages 4029–4656

Catalysis Science & Technology

www.rsc.org/catalysis

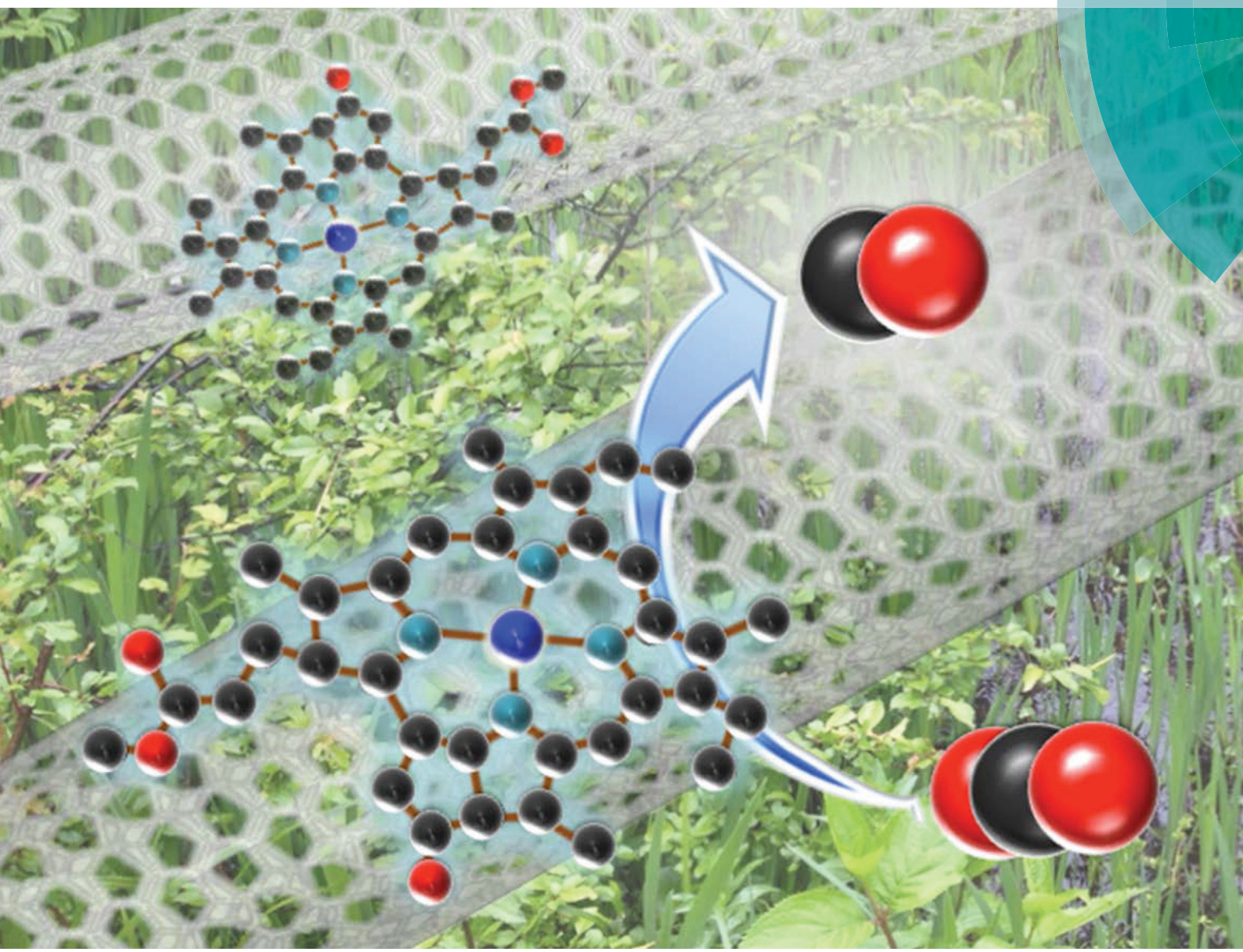

ISSN 2044-4753

ROYAL SOCIETY OF CHEMISTRY

COMMUNICATION

Kei Ohkubo, Shunichi Fukuzumi *et al.*

Photocatalytic reduction of CO_2 and H_2O to CO and H_2 with a cobalt chlorin complex adsorbed on multi-walled carbon nanotubes

175 YEARS

Catalysis Science & Technology

COMMUNICATION

View Article Online
View Journal | View Issue

Cite this: *Catal. Sci. Technol.*, 2016, 6, 4077

Received 18th February 2016,
Accepted 22nd March 2016

DOI: 10.1039/c6cy00376a

www.rsc.org/catalysis

Photocatalytic reduction of CO_2 and H_2O to CO and H_2 with a cobalt chlorin complex adsorbed on multi-walled carbon nanotubes†

Shoko Aoi,[a] Kentaro Mase,[a] Kei Ohkubo*[ab] and Shunichi Fukuzumi*[bc]

The photocatalytic reduction of CO_2 and H_2O with triethylamine occurred efficiently using a cobalt(II) chlorin complex adsorbed on multi-walled carbon nanotubes as a CO_2 reduction catalyst and $[Ru^{II}(Me_2phen)_3]^{2+}$ (Me_2phen = 4,7-dimethyl-1,10-phenanthroline) as a photocatalyst to yield CO and H_2 with a ratio of 2.4 : 1 and a high turnover number of 710.

Photocatalytic reduction of carbon dioxide (CO_2) and water (H_2O) to produce synthesis gas, which is a fuel gas mixture consisting primarily of hydrogen (H_2) and carbon monoxide (CO), has merited significant interest, because synthetic gas can be converted to liquid hydrocarbon fuels by Fischer–Tropsch processes.[1–6] The 2nd and 3rd row transition metal complexes such as Re and Ir complexes have been used as effective photocatalysts for CO_2 reduction.[7–13] The much more earth abundant metal complexes such as Co complexes have also been used as catalysts for photocatalytic CO_2 reduction.[14–21] However, the turnover number has yet to be much improved for the photocatalytic reduction of CO_2 and H_2O to produce synthetic gas with earth-abundant metal complexes.

We report herein the efficient photocatalytic reduction of CO_2 and H_2O using triethylamine (TEA) as a reductant, a cobalt(II) chlorin complex adsorbed on multi-walled carbon nanotubes (MWCNTs) as a CO_2 reduction catalyst and $[Ru^{II}(Me_2phen)_3]^{2+}$ (Me_2phen = 4,7-dimethyl-1,10-phenanthroline) as a photocatalyst in acetonitrile (MeCN) containing 5% (v/v) water to yield CO and H_2 with a 2.4 to 1.0 ratio and a high turnover number. The photocatalytic mechanism is clarified by examining each step of the catalytic cycle.

Visible light irradiation of a CO_2-saturated MeCN solution of $[Ru^{II}(Me_2phen)_3]^{2+}$, cobalt(II) chlorin complex Co^{II}(Ch) (the chemical structure is shown in Scheme 1) and TEA containing 5% (v/v) H_2O resulted in the formation of CO and H_2 as shown in Fig. 1. The optimised concentration of Co^{II}(Ch) was 40 μM and the higher concentration of Co^{II}(Ch) absorbed more light than $[Ru^{II}(Me_2phen)_3]^{2+}$ to retard the photocatalytic reaction (Fig. S1 in the ESI†). When Co^{II}(Ch) was adsorbed on MWCNTs by adding MWCNTs to the reaction solution and then stirring it (Fig. S2 in the ESI†), the yield of CO was much improved as compared with that without MWCNTs (Fig. 2). The turnover number (TON) was determined to be 710 with Co^{II}(Ch) (5.0 μM) and MWCNTs (1.0 mg) at 20 h.[25] The π–π interaction between MWCNTs and Co^{II}(Ch) may provide a suitable hydrophobic environment for the binding of CO_2 instead of proton, because the binding of CO_2 to the Co(I) complex is required for the formation of CO.[14]

The emission of $[Ru^{II}(Me_2phen)_3]^{2+*}$ was hardly quenched by Co^{II}(Ch) (Fig. S3 in the ESI†). The emission lifetime of $[Ru^{II}(Me_2phen)_3]^{2+*}$ remained the same in the presence of Co^{II}(Ch) (100 μM) as that in the absence of Co^{II}(Ch). The one-electron oxidation potential (E^*_{ox}) of $[Ru^{II}(Me_2phen)_3]^{2+*}$ was determined from the one-electron oxidation potential of the ground state (1.12 V *vs.* SCE) and the excitation energy

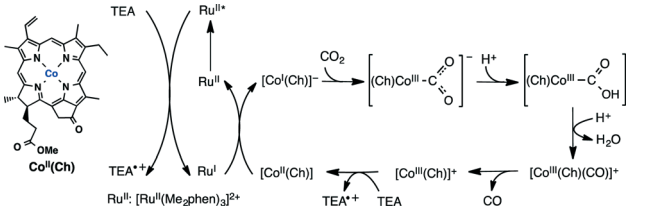

Scheme 1 Mechanism of photocatalytic CO evolution from TEA with $[Ru^{II}(Me_2phen)_3]^{2+}$ and Co^{II}(Ch).

[a] *Department of Material and Life Science, Graduate School of Engineering, Osaka University, ALCA and SENTAN, Japan Science and Technology Agency (JST), Suita, Osaka 565-0871, Japan. E-mail: ookubo@chem.eng.osaka-u.ac.jp*
[b] *Department of Chemistry and Nano Science, Ewha Womans University, Seoul 120-750, Korea. E-mail: fukuzumi@chem.eng.osaka-u.ac.jp*
[c] *Faculty of Science and Technology, Meijo University, ALCA and SENTAN, Japan Science and Technology Agency (JST), Nagoya, Aichi 468-8502, Japan*

† Electronic supplementary information (ESI) available: Experimental details and UV-vis absorption spectra (Fig. S1, S2 and S6), emission decay profiles (Fig. S3), cyclic voltammograms (Fig. S4 and S5), FTIR spectra (Fig. S7) and kinetic data (Fig. S8). See DOI: 10.1039/c6cy00376a

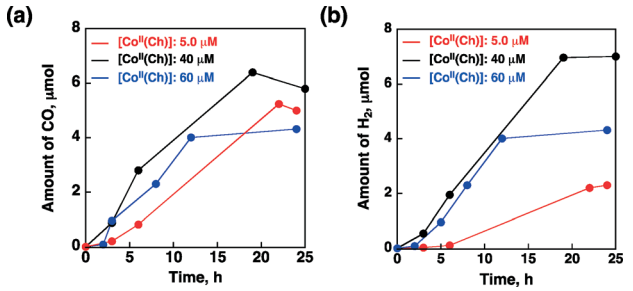

Fig. 1 Time courses of the production of (a) CO and (b) H_2 by photoirradiation of a CO_2-saturated MeCN solution of $[Ru^{II}(Me_2phen)_3]^{2+}$ (2.0 mM), $Co^{II}(Ch)$ (5.0, 40 and 60 μM) and TEA (0.50 M) containing 5% (v/v) H_2O using a xenon lamp with a cut off filter ($\lambda > 420$ nm) at 298 K.

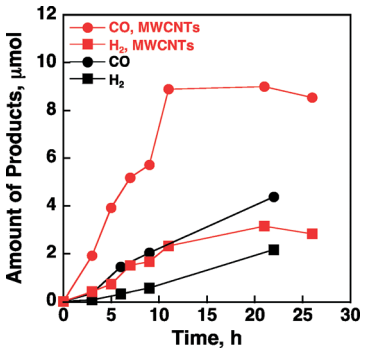

Fig. 2 Time courses of the production of CO and H_2 by photoirradiation of a CO_2-saturated MeCN solution of $[Ru^{II}(Me_2phen)_3]^{2+}$ (2.0 mM), TEA (0.50 M), $Co^{II}(Ch)$ (10 μM) adsorbed on MWCNTs (1.0 mg) (red) and $Co^{II}(Ch)$ (10 μM) without MWCNTs (black) containing 5% (v/v) H_2O using a xenon lamp with a cut off filter ($\lambda > 420$ nm) at 298 K.

(2.1 eV) to be −0.98 V *vs.* SCE.[23] The E^*_{ox} value is less negative than the one-electron reduction potential of $Co^{II}(Ch)$ (E_{red} *vs.* SCE = −0.89 V), when the electron transfer from $[Ru^{II}(Me_2phen)_3]^{2+*}$ to $Co^{II}(Ch)$ is exergonic (Fig. S4 in the ESI†).

On the other hand, the emission of $[Ru^{II}(Me_2phen)_3]^{2+*}$ was quenched by TEA by electron transfer from TEA to $[Ru^{II}(Me_2phen)_3]^{2+*}$. The one-electron reduction potential (E^*_{red}) of $[Ru^{II}(Me_2phen)_3]^{2+*}$ was determined from the one-electron reduction potential of the ground state (−1.47 V *vs.* SCE) and the excitation energy (2.1 eV) to be 0.67 V *vs.* SCE. Because the E_{ox} value of TEA (0.74 V *vs.* SCE), which was determined by second harmonic ac voltammetry (SHACV; Fig. S5 in the ESI†), is more positive than the E^*_{red} value, the electron transfer from TEA to $[Ru^{II}(Me_2phen)_3]^{2+*}$ is slightly endergonic. The rate constant of electron transfer from TEA to $[Ru^{II}(Me_2phen)_3]^{2+*}$ was determined from the Stern–Volmer plot (Fig. 3) to be 1.7×10^6 M^{-1} s^{-1} in MeCN at 298 K. The quantum yield of the photocatalytic reduction of CO_2 to CO under photoirradiation of light at $\lambda = 450$ nm was determined to be 0.10% using a ferric oxalate actinometer (see the Experimental section in the ESI†).

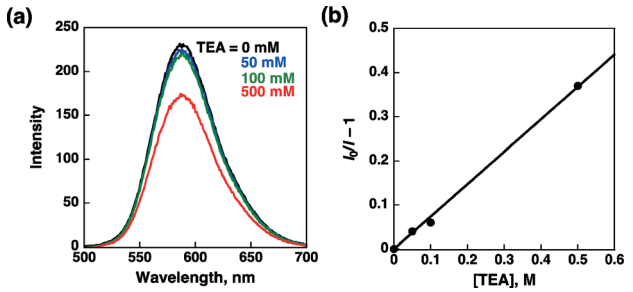

Fig. 3 (a) Emission spectra of $[Ru^{II}(Me_2phen)_3]^{2+}$ (8.8 μM) with various concentrations of TEA (0–0.50 M) in deaerated MeCN containing 5% (v/v) H_2O at 298 K. (b) Stern–Volmer plot.

The photocatalytic mechanism of the CO_2 reduction is shown in Scheme 1. Upon photoexcitation of $[Ru^{II}(Me_2phen)_3]^{2+}$, electron transfer from TEA to $[Ru^{II}(Me_2phen)_3]^{2+*}$ occurs to produce a TEA radical cation and $[Ru(Me_2phen)_3]^{+}$, the latter of which reduces $Co^{II}(Ch)$ to $[Co^{I}(Ch)]^{-}$. The TEA radical cation may be deprotonated to produce a neutral radical that may be further oxidized. Thus, the endergonic electron transfer from TEA to $[Ru^{II}(Me_2phen)_3]^{2+*}$ (*vide supra*) is irreversible. We have previously reported that CO_2 is reduced to CO when $Co^{II}(Ch)$ is electrochemically reduced to $[Co^{I}(Ch)]^{-}$.[22] At the same time $[Co^{I}(Ch)]^{-}$ was reported to react with H^+ to produce the hydride complex ($[Co^{III}(H)(Ch)]$), which reacts with H^+ to produce H_2.[24] $[Co^{III}(H)(Ch)]$ is also an intermediate for H_2 evolution in the photocatalytic reduction of H_2O to H_2.[26]

In order to examine the reaction of $[Co^{I}(Ch)]^{-}$ with CO_2, $[Co^{I}(Ch)]^{-}$ was prepared independently by the one-electron reduction of $Co^{II}(Ch)$ with decamethylcobaltocene $[Co(Cp^*)_2]$ in MeCN as reported previously.[24] The UV-vis absorption band of $[Co^{I}(Ch)]^{-}$ (green line in Fig. 4a; $\lambda_{max} = 510$ nm) decreased, accompanied by an increase in absorbance at 660 nm due to $[Co^{III}(Ch)(CO_2)]^{-}$ (blue line) at 65 ms upon introduction of CO_2 by mixing.[27] Then, this absorption band finally blue shifted to $\lambda_{max} = 652$ nm, which is due to $[Co^{III}(Ch)(CO)]^{+}$

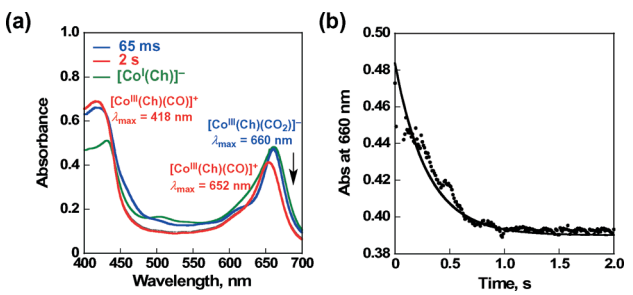

Fig. 4 (a) UV-vis absorption spectral changes of $[Co^{I}(Ch)]^{-}$ (20 μM) upon introduction of CO_2-saturated MeCN containing 5% (v/v) H_2O at 298 K. The blue and red lines show the spectra taken at 65 ms and 2 s after mixing, respectively. The green line shows the UV-vis absorption spectrum of $[Co^{I}(Ch)]^{-}$ (15 μM) formed by the electron-transfer reduction of $Co^{II}(Ch)$ (15 μM) with $Co(Cp^*)_2$ (300 μM) in deaerated MeCN at 298 K.[24] (b) Decay time profile of absorbance at 660 nm due to $[Co^{III}(Ch)(CO_2)]^{-}$.

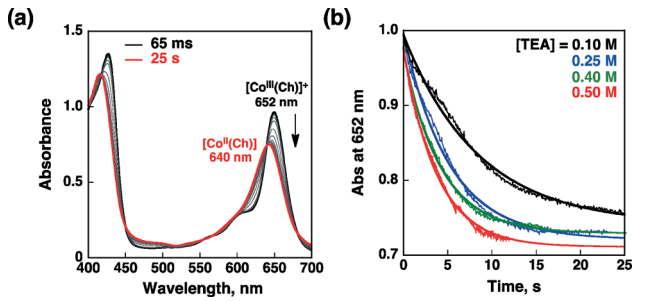

Fig. 5 (a) UV-vis absorption spectral changes in the electron-transfer reduction of $[Co^{III}(Ch)]^+$ (20 μM) with TEA (0.10 M) in deaerated MeCN containing 5% (v/v) H_2O at 298 K at 65 ms and 25 s after mixing. (b) Decay time profiles of absorbance at 652 nm due to $[Co^{III}(Ch)]^+$ in the presence of various concentrations of TEA in deaerated MeCN containing 5% (v/v) H_2O at 298 K.

(red line). This absorption band matched with that of $[Co^{III}(Ch)(CO)]^+$ which was produced by introducing CO to $[Co^{III}(Ch)]^+$ in MeCN (Fig. S6 in the ESI†). When N_2 was introduced to $[Co^{III}(Ch)(CO)]^+$, the spectrum returned to $[Co^{III}(Ch)]^+$. This indicates that the binding of CO to $[Co^{III}(Ch)]^+$ is reversible. The CO stretching frequency of $[Co^{III}(Ch)(CO)]^+$ was also measured in MeCN under an appropriate CO pressure (Fig. S7 in the ESI†). *ν*CO is located at 2158 cm^{-1}, which is nearly the same as the "free" CO molecule (*ν*CO = 2155 cm^{-1}),[28] suggesting a weak reversible coordination. Finally, $[Co^{III}(Ch)(CO_2)]^-$ was converted to $[Co^{III}(Ch)]^+$ and CO by protonation with dehydration (Scheme 1). The rate constant of the formation of $[Co^{III}(Ch)(CO)]^+$ was determined from the change in absorbance at 660 nm to be 3.4 s^{-1} (Fig. 4b).

$[Co^{III}(Ch)]^+$, which was prepared by one-electron oxidation of $Co^{II}(Ch)$ with $(p\text{-}BrC_6H_4)_3N^{\cdot+}SbCl_6^-$, was thermally reduced by TEA to produce $Co^{II}(Ch)$ (Scheme 1) as shown in Fig. 5a. The rate of reduction of $[Co^{III}(Ch)]^+$ by a large excess of TEA obeyed first-order kinetics and the pseudo-first-order rate constant was proportional to the concentration of TEA. From the slope of the linear plot of the pseudo-first-order rate constant *vs.* concentration of TEA, the second-order rate constant was determined to be 0.64 M^{-1} s^{-1} (Fig. S8 in the ESI†).

In conclusion, $Co^{II}(Ch)$ adsorbed on MWCNTs acts as an efficient catalyst for photocatalytic CO_2 reduction to CO as well as H_2 evolution from TEA in MeCN containing 5% (v/v) water. The present study paves a new way to produce synthetic gas from CO_2 and H_2O using an earth-abundant metal complex catalyst for CO_2 reduction under visible light irradiation.

Acknowledgements

This work was supported by Grants-in-Aid (no. 26620154 and 26288037 to K. O.) and a JSPS fellowship (No. 25727 to K. M.) from the Ministry of Education, Culture, Sports, Science and Technology (MEXT), and by ALCA and SENTAN projects from JST, Japan (to S. F.).

Notes and references

1 M. Aresta, A. Dibenedetto and A. Angelini, *Chem. Rev.*, 2014, **114**, 1709.
2 Q. Yi, W. Li, J. Feng and K. Xie, *Chem. Soc. Rev.*, 2015, **44**, 5409.
3 J. A. Herron, J. Kim, A. A. Upadhye, G. W. Huber and C. T. Maravelias, *Energy Environ. Sci.*, 2015, **8**, 126.
4 M. E. Dry, *Catal. Today*, 2002, **71**, 227.
5 E. V. Kondratenko, G. Mul, J. Baltrusaitis, G. O. Larrazábal and J. Pérez-Ramírez, *Energy Environ. Sci.*, 2013, **6**, 3112.
6 S. Berardi, S. Drouet, L. Francàs, C. Gimbert-Suriñach, M. Guttentag, C. Richmond, T. Stoll and A. Llobet, *Chem. Soc. Rev.*, 2014, **43**, 7501.
7 E.-G. Ha, J.-A. Chang, S.-M. Byun, C. Pac, D.-M. Jang, J. Park and S. O. Kang, *Chem. Commun.*, 2014, **50**, 4462.
8 (*a*) G. Sahara and O. Ishitani, *Inorg. Chem.*, 2015, **54**, 5096; (*b*) H. Takeda and O. Ishitani, *Coord. Chem. Rev.*, 2010, **254**, 346; (*c*) Y. Yamazaki, H. Takeda and O. Ishitani, *J. Photochem. Photobiol., C*, 2015, **25**, 106–137.
9 L. M. Kiefer, J. T. King and K. J. Kubarych, *Acc. Chem. Res.*, 2015, **48**, 1123.
10 M. D. Sampson, J. D. Froehlich, J. M. Smieja, E. E. Benson, I. D. Sharp and C. P. Kubiak, *Energy Environ. Sci.*, 2013, **6**, 3748.
11 R. O. Reithmeier, S. Meister, B. Rieger, A. Siebel, M. Tschurl, U. Heiz and E. Herdtweck, *Dalton Trans.*, 2014, **43**, 13259.
12 D. J. Boston, Y. M. Franco Pachón, R. O. Lezna, N. R. de Tacconi and F. M. Macdonnell, *Inorg. Chem.*, 2014, **53**, 6544.
13 S. Sato, T. Morikawa, T. Kajino and O. Ishitani, *Angew. Chem., Int. Ed.*, 2013, **52**, 988.
14 (*a*) G. F. Manbeck, E. Fujita and J. Porphyrins, *Phthalocyanines*, 2015, **19**, 45; (*b*) A. J. Morris, G. J. Meyer and E. Fujita, *Acc. Chem. Res.*, 2009, **42**, 1983; (*c*) D. Behar, T. Dhanasekaran, P. Neta, C. M. Hosten, D. Ejeh, P. Hambright and E. Fujita, *J. Phys. Chem. A*, 1998, **102**, 2870; (*d*) J. Grodkowski, P. Neta, E. Fujita, A. Mahammed, L. Simkhovich and Z. Gross, *J. Phys. Chem. A*, 2002, **106**, 4772.
15 J. Bonin, M. Robert and M. Routier, *J. Am. Chem. Soc.*, 2014, **136**, 16768.
16 L. Chen, Z. Guo, X.-G. Wei, C. Gallenkamp, J. Bonin, E. Anxolabéhère-Mallart, K.-C. Lau, T.-C. Lau and M. Robert, *J. Am. Chem. Soc.*, 2015, **137**, 10918.
17 S. Kumar, M. Y. Wani, C. T. Arranja, J. de A. e Silva, B. Avula and A. J. F. N. Sobral, *J. Mater. Chem. A*, 2015, **3**, 19615.
18 J. Lin, Z. Pan and X. Wang, *ACS Sustainable Chem. Eng.*, 2014, **2**, 353.
19 C. Matlachowski and M. Schwalbe, *Dalton Trans.*, 2015, **44**, 6480.
20 J. Bonin, M. Chaussemier, M. Robert and M. Routier, *ChemCatChem*, 2014, **6**, 3200.
21 P. Kumar, A. Kumar, C. Joshi, R. Singh, S. Saran and S. L. Jain, *RSC Adv.*, 2015, **5**, 42414.
22 S. Aoi, K. Mase, K. Ohkubo and S. Fukuzumi, *Chem. Commun.*, 2015, **51**, 10226.
23 S. Kato, J. Jung, T. Suenobu and S. Fukuzumi, *Energy Environ. Sci.*, 2013, **6**, 3756.

24 S. Aoi, K. Mase, K. Ohkubo and S. Fukuzumi, *Chem. Commun.*, 2015, **51**, 15145.

25 The TON for CO formation was improved by the adsorption of the cobalt chlorin complex on MWCNTs, because two $[Co^{I}(Ch)]^{-}$ molecules are located close to each other where the two-electron reduction of CO_2 to CO may occur. The optimized amount of MWCNTs was 1.0 mg under the present experimental conditions, because the amounts of CO and H_2 produced in the present photocatalytic system became smaller when 0.5 mg and 1.5 mg of MWCNTs were employed instead of 1.0 mg of MWCNTs.

26 No Co(0) species was produced because a Co(I)/Co(0) couple was not observed in CV measurements. Thus, the catalytically active species for proton reduction maybe Co(III)–H.[24].

27 An X-ray absorption near-edge spectroscopy (XANES) study of the Co(III)–CO_2 adducts clearly indicated a significant charge-transfer from Co(I) to the bound CO_2 (see: E. Fujita, L. R. Furenlid and M. W. Renner, *J. Am. Chem. Soc.*, 1997, **119**, 4549).

28 K. Nakamoto, *Infrared and Raman Spectra of Inorganic and Coordination Compounds*, Wiley-Interscience, New York, 1978, 3rd edn, Part III.

